FACTA UNIVERSITATIS
Series: **Mechanical Engineering**

Supplementary document – additional figures and tables

STRUCTURAL AND MECHANICAL CHARACTERIZATION OF 3D-PRINTED PLA-REINFORCED CONCRETE BEAMS VIA FINITE ELEMENT MODELING AND DIC-BASED BENDING TESTS

Hanna Csótár[1], Szabolcs Szalai[1], Péter Grubits[2], Dmytro Kurhan[3], Mykola Sysyn[4], Szabolcs Fischer[1]

[1]Széchenyi István University, Central Campus, Hungary
[2]Széchenyi István University,
Department of Structural and Geotechnical Engineering, Hungary
[3]Ukrainian State University of Science and Technologies,
Department of Transport Infrastructure, Ukraine
[4]Technical University Dresden,
Department of Planning and Design of Railway Infrastructure, Germany

Table S1 Printing parameters of the specimens (where the upper value denotes the bed temperature, and the lower value denotes the nozzle temperature)

Material	Designation	Manufacturer	Recommended [°C]	Applied [°C]
Acrylonitrile-Butadiene-Styrene	ABS	Filaticum	80-95	90
			260-290	260
Gypsum PLA	GYP	Filaticum	55-70	90
			190-215	200
PLA High Impact	HI	Filaticum	45-65	60
			190-210	200
Engineering PLA	ENG	Filaticum	65-75	75
			215-240	225
Electrical Electrostatic Discharge PLA	ESD	Filaticum	55-70	60
			190-215	200

Table S2 Mechanical parameters of the 3D printed materials

Designation (DES)	**Manufacturer**	**Izod impact strength [kJ/m²]**	**Tensile strength [MPa]**	**Young's modulus**	**Poisson's ratio (ν)**
ABS	Filaticum	5.2	32.5	1800	0.35-0.40
GYP	Filaticum	2.9	25.0	1400	0.24-0.39
HI	EUMAKERS	4.0	36.0	3200	0.32-0.36
ENG	Filaticum	3.7	32.2	2500	0.35
ESD	3DXTECH	under testing	55.0	2560	0.35

Table S3 List of the measuring instruments and programs used

Category	Device / Software	Manufacturer	Location	Role
Optical measurement	GOM ARAMIS 5M stereo camera system	GOM	Braunschweig, Germany	12 MP cameras, DIC for deformation analysis
	CP20 calibration plate	GOM	Braunschweig, Germany	Calibration target for stereo camera system
	ARAMIS 2018 software	GOM	Braunschweig, Germany	DIC data processing

Table S4 List of the measuring instruments and programs used (cont.)

Load and displacement measurement	W5TK-7777-K travel transmitter	HBM	Germany	Displacement transducer
	S9861-20 kN S-type load cell	Kaliber Kft.	Hungary	Force measurement
Material testing	Matest C278 vibrating table	Matest S.p.A.	Arcore, Italy	Vibrating platform for specimen preparation
	40×40 mm^2 E170 crushing pad	-	-	Loading pad for compression tests
3D Printing	Creality Ender 3 – V2 desktop FDM printer	Creality 3D Technology Co., Ltd.	Shenzhen, China	Fused Deposition Modeling (FDM)
	UltiMaker Cura 5.30 slicing software	UltiMaker	-	Slicing software
Numerical simulation	Abaqus/CAE 2018 FEM software	Dassault Systemes	-	Finite Element Modelling (FEM)

Table S5 Tensile strength of concrete samples

DES	***L***	***d₁***	***d₂***	**Mass**	**ρ**	***F***	***f_cf***	***E***
	[mm]	**[mm]**	**[mm]**	**[g]**	**[kg/m³]**	**[kN]**	**[N/mm²]**	**[N/mm²]**
C1	159.1	40	39.6	583.74	2.316	4.68	8.39	732.62
C2	159.2	40.1	39.9	592.43	2.325	3.35	5.90	436.16
C3	160.5	39.9	40.1	589.37	2.295	3.87	6.78	790.99
C4	160.4	40.0	39.8	592.13	2.318	3.94	6.99	881.82
C5	160.3	39.9	40.0	589.36	2.304	3.83	6.75	973.35

Table S6 Compressive strength of concrete samples

DES		***F***	**Compressive strength**
		[kN]	**[N/mm^2]**
C1	C1 — A	123.90	77.44
	C1 — B	132.50	82.81
C2	C2 — A	128.01	80.01
	C2 — B	138.00	86.25
C3	C3 — A	134.45	84.03
	C3 — B	125.53	78.46
C4	C4 — A	129.96	81.22
	C4 — B	117.79	73.62
C5	C5 — A	132.99	83.12
	C5 — B	133.44	83.40

Table S7 Splitting-tensile strength of cylinder samples

DES	***L***	***d***	**Mass**	***ρ***	***F***	f_{ct}
	[mm]	**[mm]**	**[g]**	**[kg/m³]**	**[kN]**	**[N/mm²]**
Sp1	37.3	36.8	90.90	2.291	14.37	6.66
Sp2	37.6	36.7	91.14	2.291	17.08	7.88
Sp3	37.2	36.6	91.45	2.336	10.42	4.87
Sp4	37.6	36.6	91.48	2.312	8.66	4.01
Sp5	37.4	36.7	91.31	2.308	11.50	5.33
Sp6	37.5	36.6	91.06	2.308	11.57	5.36

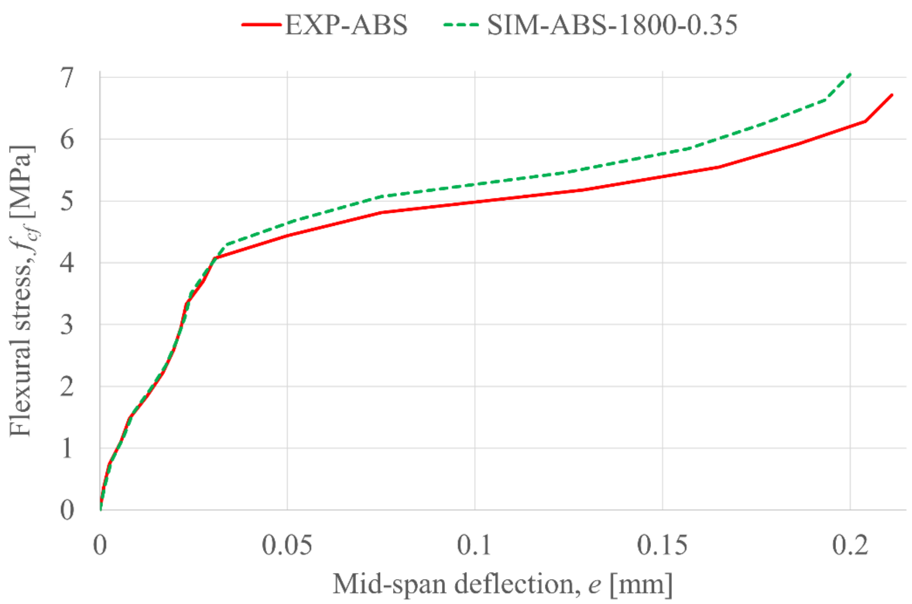

Fig. S1 Comparisons of simulation and experimental results – ABS reinforcement

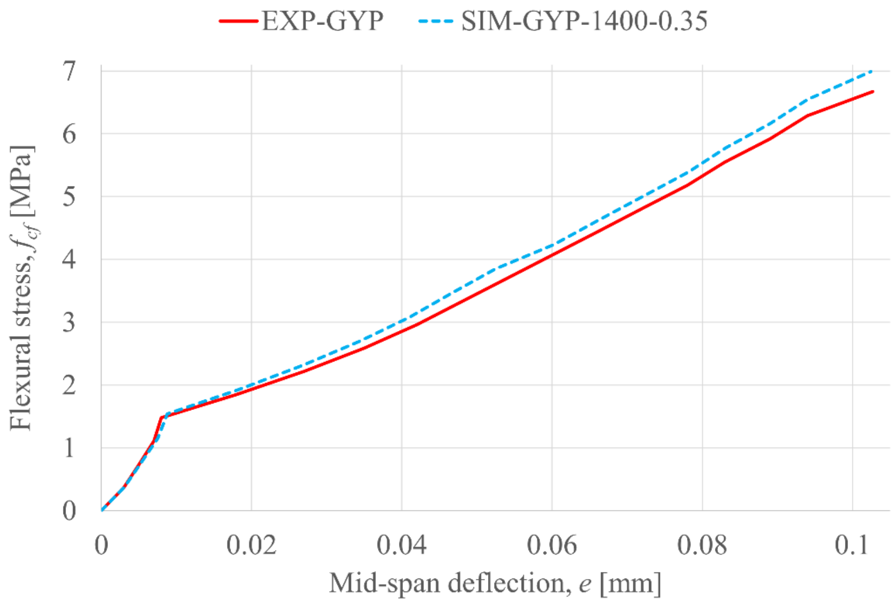

Fig. S2 Comparisons of simulation and experimental results – GYP reinforcement

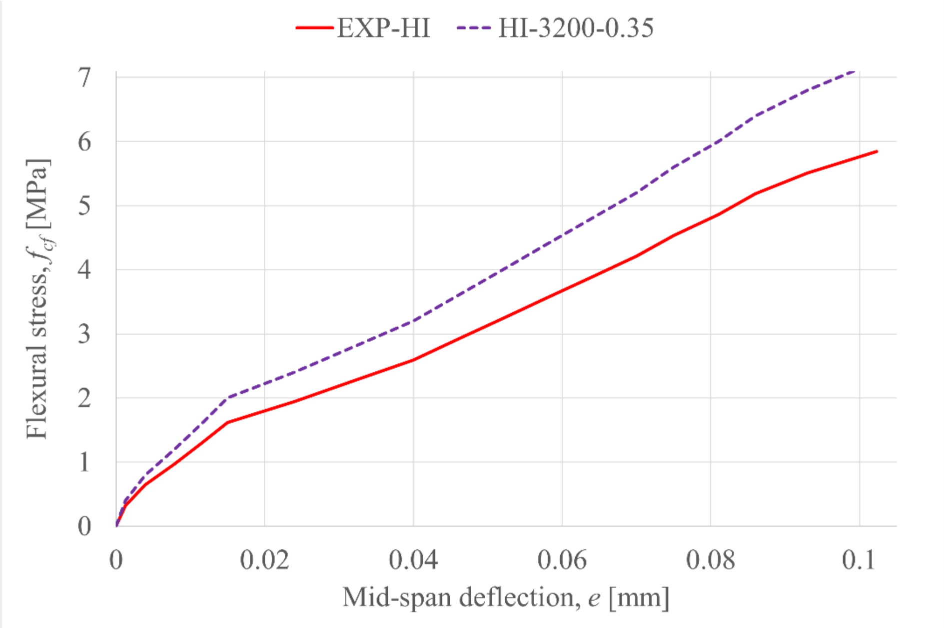

Fig. S3 Comparisons of simulation and experimental results – HI reinforcement

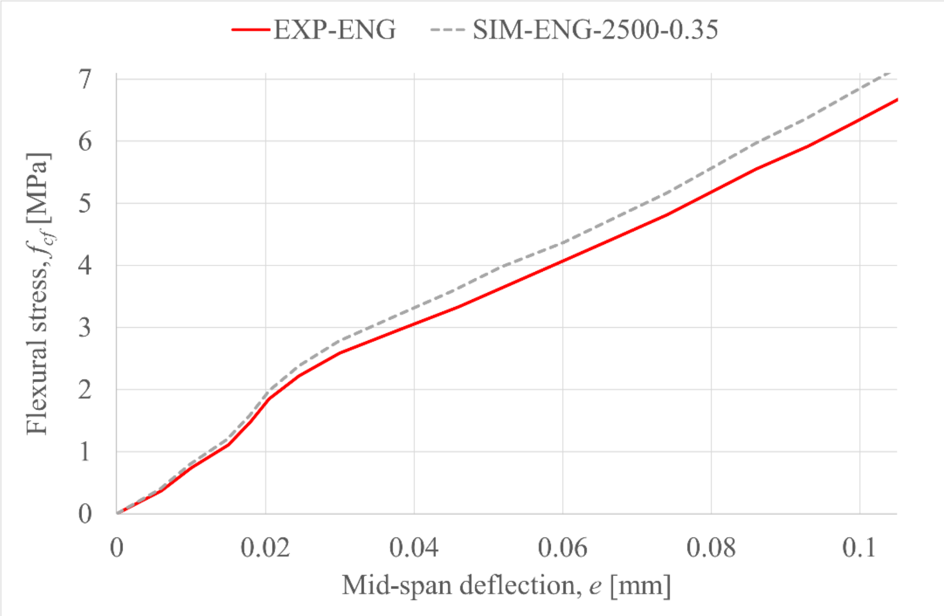

Fig. S4 Comparisons of simulation and experimental results – ENG reinforcement

Table S8 Deflection results of the experimental and numerical measurements (where the load factors of the specimens in kN were: ABS = 0.9326, GYP = 0.9269, HI = 0.8115, ENG = 0.9277.)

Case	**Results of the vertical deflection**
ABS (Exp.)	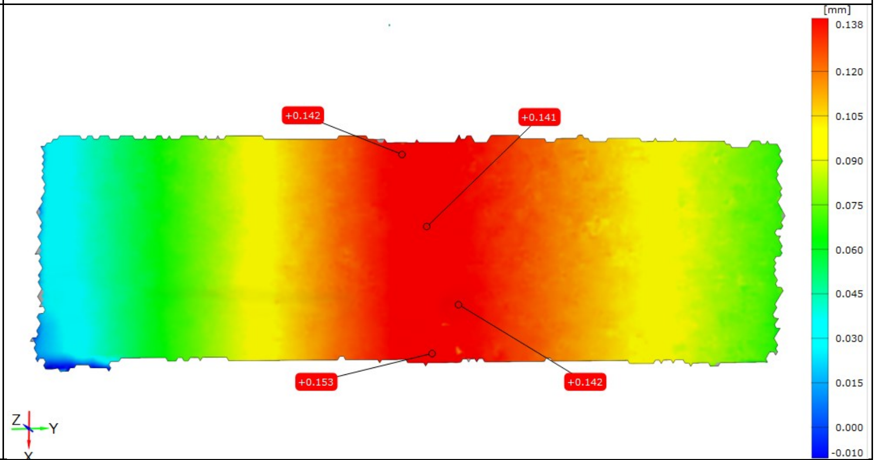
ABS (Num.)	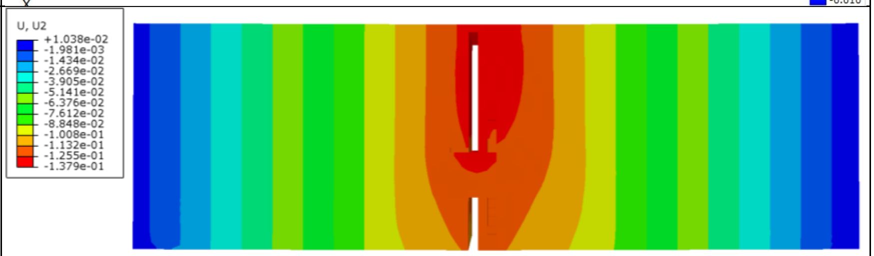
GYP (Exp.)	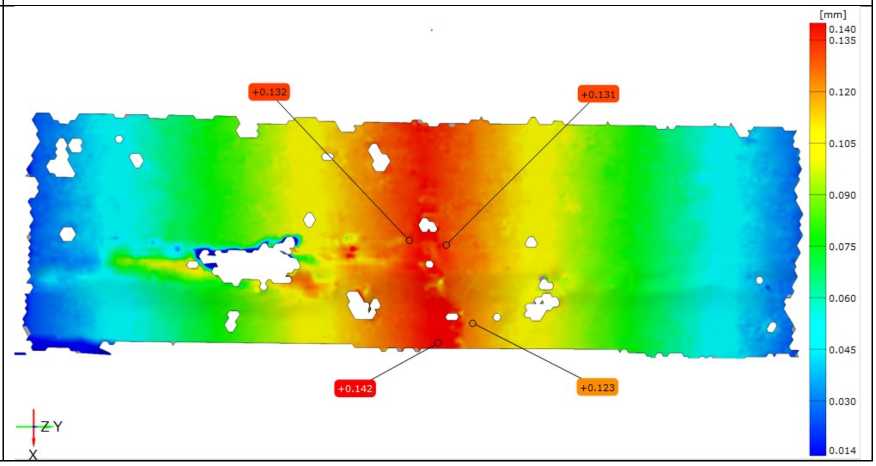

Table S9 Deflection results of the experimental and numerical measurements (where the load factors of the specimens in kN were: ABS = 0.9326, GYP = 0.9269, HI = 0.8115, ENG = 0.9277.) (cont.)

Case	Results of the vertical deflection
ABS (Exp.)	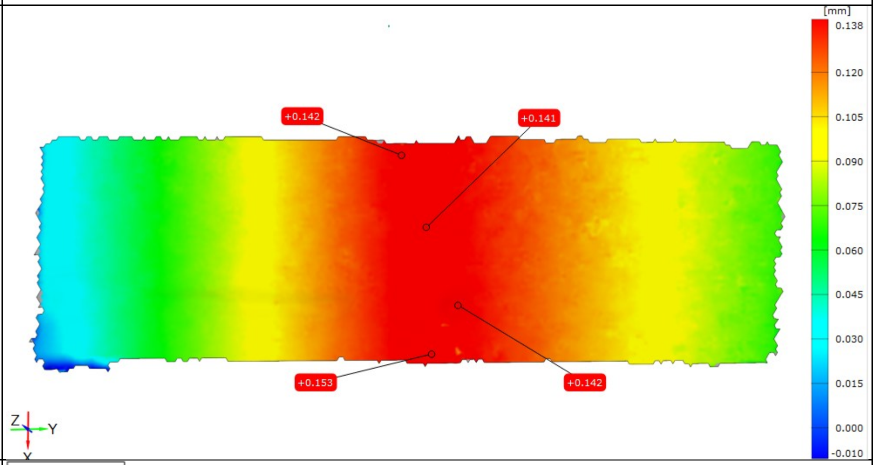
ABS (Num.)	
GYP (Exp.)	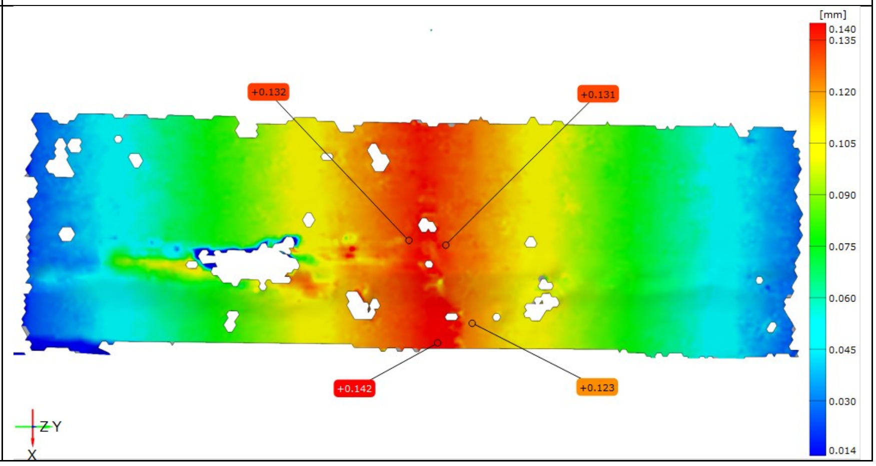

Table S10 Deflection results of the experimental and numerical measurements (where the load factors of the specimens in kN were: ABS = 0.9326, GYP = 0.9269, HI = 0.8115, ENG = 0.9277.) (cont.)

Case	**Results of the vertical deflection**
ENG (Num.)	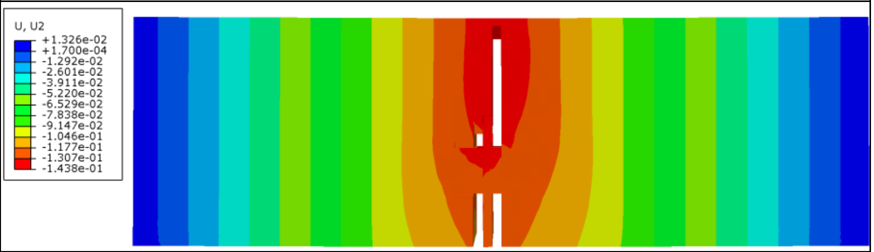

Table S11 Numerical results – Reinforcement part (red–fully damaged area, blue–undamaged area)

Case	Results of the vertical deflection
ABS	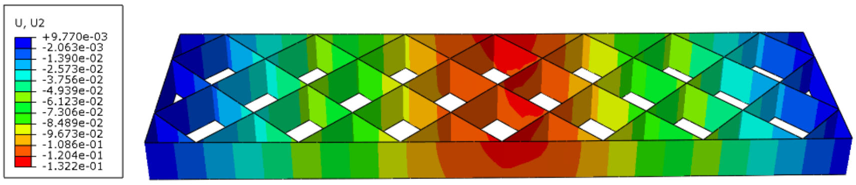
GYP	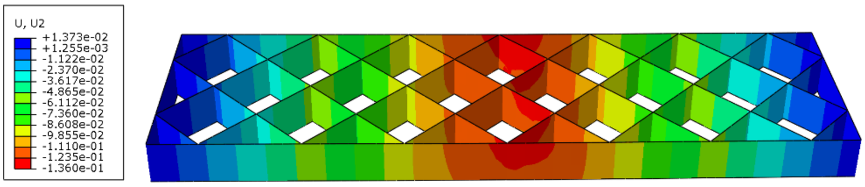
HI	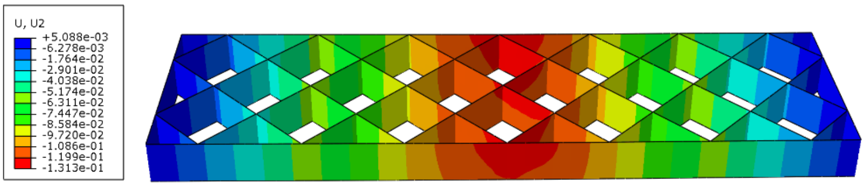
ENG	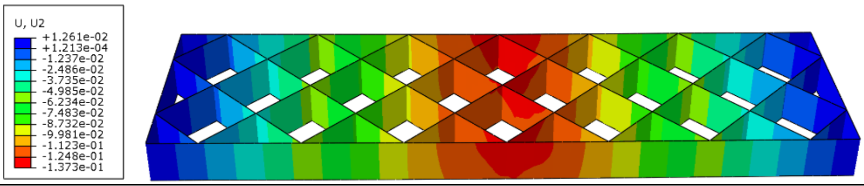

Table S12 Influence of the thickness modification of ABS reinforcement

Case	**Thickness value [mm]**	**Vertical deflection factor value, *e* [mm]**	**Flexural stress, f_{cf} [MPa]**
EXP-ABS	0.4	0.211	6.715
ABS-G-0.2	0.2	0.1999	6.785
ABS-G-0.4	0.4	0.1999	6.886
ABS-G-0.8	0.8	0.1999	7.044
ABS-T-0.2	0.2	0.1999	6.899
ABS-T-0.4	0.4	0.2019	7.225
ABS-T-0.8	0.8	0.2019	7.477

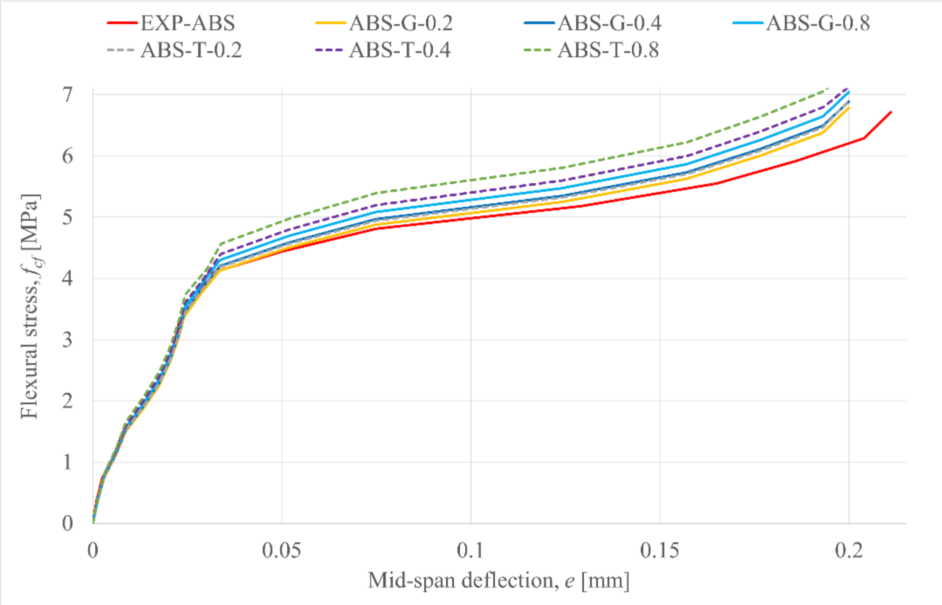

Fig. S5 Impact of changing the infill pattern and the thickness of the ABS reinforcement

Table S13 Influence of the thickness modification of ABS reinforcement

Case	***f_{cf}* [MPa]**	***e* [mm]**	**SSE**	**MAE**	**RMSE**	**R^2**
EXP-ABS	6.715	0.211	ref.	ref.	ref.	ref.
ABS-G-0.2	6.785	0.1999	0.05	–0.40	0.05	1.00
ABS-G-0.4	6.886	0.1999	0.28	–0.10	0.12	0.99
ABS-G-0.8	7.044	0.1999	0.89	–0.19	0.22	0.99
ABS-T-0.2	6.899	0.1999	0.21	–0.09	0.10	1.00
ABS-T-0.4	7.225	0.2019	1.87	–0.27	0.31	0.99
ABS-T-0.8	7.477	0.2019	4.19	–0.40	0.47	0.99

Table S14 Influence of the thickness modification of GYP reinforcement

Case	Thickness value [mm]	Vertical deflection factor value, *e* [mm]	Flexural stress, f_{cf} [MPa]
EXP-GYP	0.4	0.1027	6.674
GYP-G-0.2	0.2	0.1024	6.762
GYP-G-0.4	0.4	0.1024	6.844
GYP-G-0.8	0.8	0.1024	6.992
GYP-T-0.2	0.2	0.1024	6.862
GYP-T-0.4	0.4	0.1044	7.162
GYP-T-0.8	0.8	0.1024	7.249

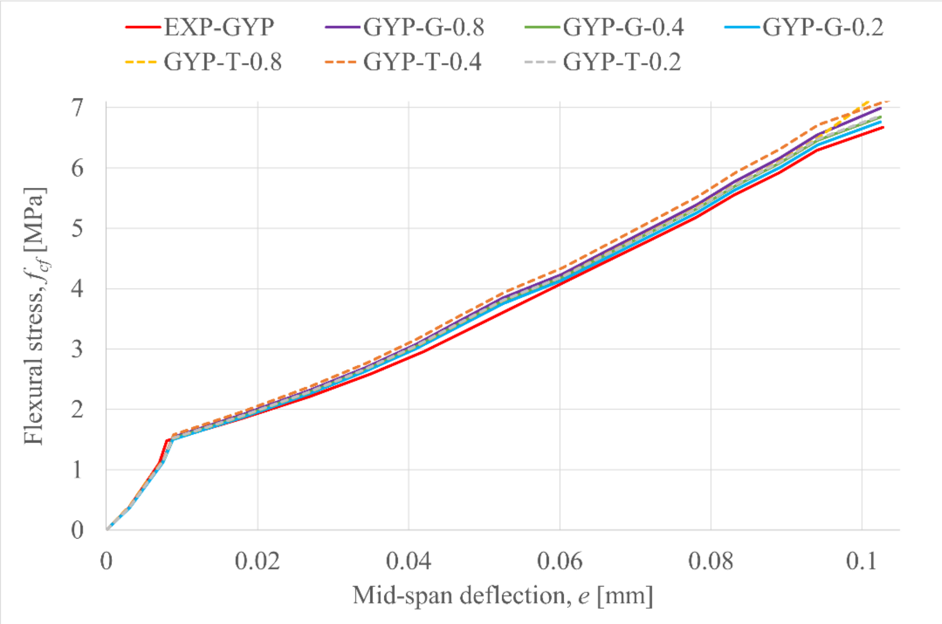

Fig. S6 Impact of changing the infill pattern and the thickness of the GYP reinforcement

Table S15 Influence of the thickness modification of GYP reinforcement

Case	f_{cf} [MPa]	*e* [mm]	SSE	MAE	RMSE	R^2
EXP-GYP	6.674	0.1027	ref.	ref.	ref.	ref.
GYP-G-0.2	6.762	0.1024	0.06	–0.05	0.06	1
GYP-G-0.4	6.844	0.1024	0.21	–0.08	0.1	1
GYP-G-0.8	6.992	0.1024	0.5	–0.14	0.16	0.99
GYP-T-0.2	6.862	0.1024	0.25	–0.09	0.12	1
GYP-T-0.4	7.162	0.1044	1.35	–0.23	0.27	0.99
GYP-T-0.8	7.249	0.1024	0.51	–0.11	0.16	0.99

Table S16 Influence of the thickness modification of HI reinforcement

Case	Thickness value [mm]	Vertical deflection factor value, *e* [mm]	Flexural stress, f_{cf} [MPa]
EXP-HI	0.4	0.1023	5.843
HI-G-0.2	0.2	0.1023	6.865
HI-G-0.4	0.4	0.1023	7.011
HI -G-0.8	0.8	0.1023	7.245
HI-T-0.2	0.2	0.1023	7.192
HI-T-0.4	0.4	0.1023	7.426
HI-T-0.8	0.8	0.1023	7.774

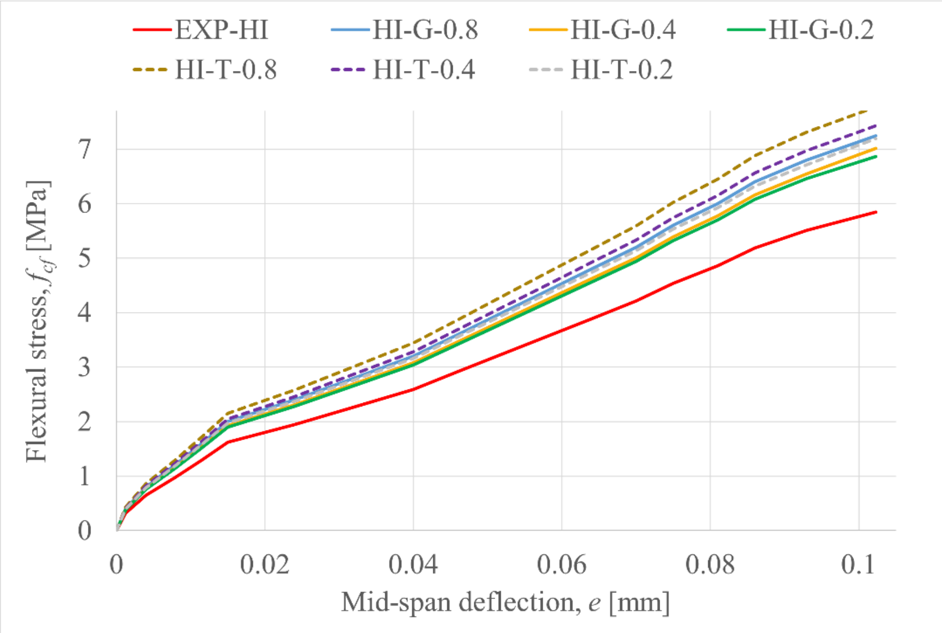

Fig. S7 Impact of changing the infill pattern and the thickness of the HI reinforcement

Table S17 Discrepancies between simulation of HI reinforcement and experimental results (first row shows the reference values for experimental data)

Case	f_{cf} [MPa]	e [mm]	SSE	MAE	RMSE	R^2
EXP-HI	5.843	0.1023	ref.	ref.	ref.	ref.
HI-G-0.2	6.865	0.1023	6.64	–0.5	0.59	1
HI-G-0.4	7.011	0.1023	8.01	–0.55	0.65	0.99
HI-G-0.8	7.245	0.1023	12.28	–0.7	0.8	0.99
HI-T-0.2	7.192	0.1023	10.82	–0.6	0.75	0.99
HI-T-0.4	7.426	0.1023	15.71	–0.78	0.91	0.99
HI-T-0.8	7.774	0.1023	23.79	–0.95	1.12	1

Table S18 Influence of the thickness modification of ENG reinforcement

Case	Thickness value [mm]	Vertical deflection factor value, *e* [mm]	Flexural stress, f_{cf} [MPa]
EXP-ENG	0.4	0.1052	6.679
ENG-G-0.2	0.2	0.1047	6.826
ENG-G-0.4	0.4	0.1047	6.949
ENG-G-0.8	0.8	0.1047	7.156
ENG-T-0.2	0.2	0.1067	7.112
ENG-T-0.4	0.4	0.1067	7.333
ENG-T-0.8	0.8	0.1067	7.634

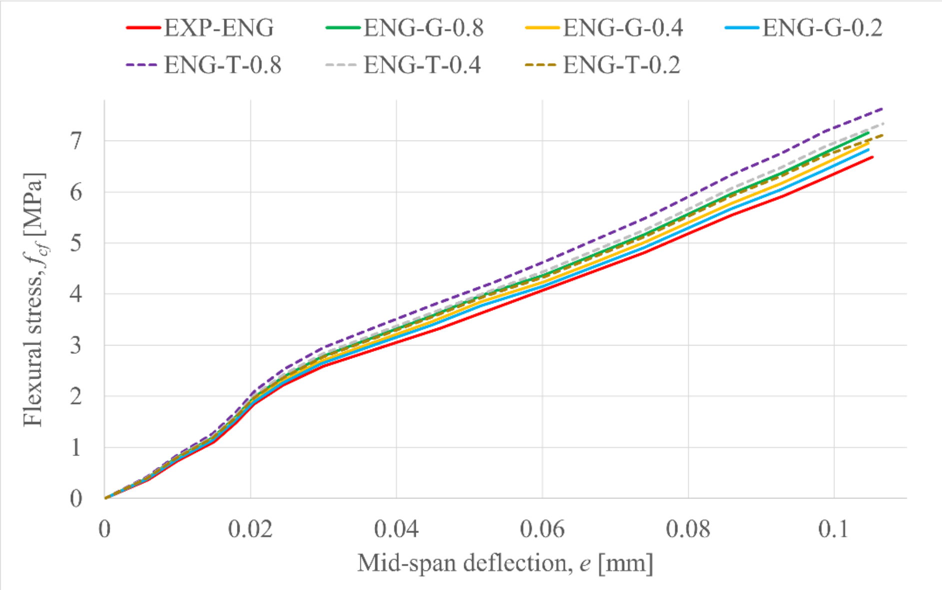

Fig. S8 Impact of changing the infill pattern and the thickness of the ENG reinforcement

Table S19 Discrepancies between simulation of ENG reinforcement and experimental results (first row shows the reference values for experimental data)

Case	f_{cf} [MPa]	*e* [mm]	SSE	MAE	RMSE	R^2
EXP-ENG	6.679	0.1052	ref.	ref.	ref.	ref.
ENG-G-0.2	6.826	0.1047	0.12	–0.07	0.08	1
ENG-G-0.4	6.949	0.1047	0.47	–0.14	0.16	1
ENG-G-0.8	7.156	0.1047	1.58	–0.25	0.29	1
ENG-T-0.2	7.112	0.1067	1.31	–0.22	0.26	1
ENG-T-0.4	7.333	0.1067	2.61	–0.32	0.37	1
ENG-T-0.8	7.634	0.1067	5.83	–0.5	0.55	1

Table S20 Impact of Poisson's ratio and Young's modulus in the case of HI reinforcement (first row shows the reference values for experimental data)

E **[MPa]**	***ν***	***f_{cf}*** **[MPa]**	***e*** **[mm]**	**SSE**	**MAE**	**RMSE**	**R^2**
-	-	5.843	0.1023	ref.	ref.	ref.	ref.
3200	0.32	6.862	0.1023	6.64	–0.5	0.59	1
3200	0.33	6.886	0.1023	6.69	–0.5	0.59	1
3200	0.34	6.869	0.1023	6.65	–0.5	0.59	1
3200	0.35	6.865	0.1023	6.64	–0.5	0.59	1
3200	0.36	6.869	0.1023	6.64	–0.5	0.59	1
3000	0.35	6.852	0.1023	6.62	–0.5	0.59	1
2800	0.35	6.844	0.1023	6.59	–0.5	0.59	1
2600	0.35	6.839	0.1023	6.29	–0.49	0.58	1
2400	0.35	6.815	0.1023	6.25	–0.49	0.57	1
2200	0.35	6.811	0.1023	6.14	–0.48	0.56	1
2000	0.35	6.804	0.1023	6.03	–0.48	0.56	1
1800	0.35	6.779	0.1023	5.79	–0.47	0.55	1

Table S21 Numerical results from infill and grid modification of ESD reinforcement – Beam part with embedded reinforcement

DES	Results of the vertical deflection
ESD-G-0.2	
ESD-G-0.4	
ESD-G-0.8	
ESD-T-0.2	

Table S22 Numerical results from infill and grid modification of ESD reinforcement – Beam part with embedded reinforcement (cont.)

DES	Results of the vertical deflection
ESD-T-0.4	
ESD-T-0.8